NeuroImage **12,** 71–84 (2000)
doi:10.1006/nimg.2000.0589, available online at http://www.idealibrary.com on IDEAL®

Spatiotemporal Analysis of Neuromagnetic Events Underlying the Emergence of Coordinative Instabilities

A. Fuchs,* J. M. Mayville,* D. Cheyne,† H. Weinberg,† L. Deecke,‡ and J. A. S. Kelso*

**Center for Complex Systems and Brain Sciences, Florida Atlantic University, Boca Raton, Florida 33431;*
†Brain Behavior Laboratory, Simon Fraser University, Burnaby, British Columbia, Canada; and
‡Department of Neurology, General Hospital Vienna, A-1090 Vienna, Austria

Received November 16, 1999

A full-head 143-channel superconducting quantum interference device was used to study changes occurring in the magnetic activity of the human brain during performance of an auditory–motor coordination task in which the rate of coordination was systematically increased. Previous research using the same task paradigm demonstrated that spontaneous switches in timing behavior that arise with higher coordination rates are accompanied by qualitative changes in spatiotemporal brain activity measured by electro- and magnetoencephalography. Here we show how these patterns can be decomposed into basic physiological events, i.e., evoked brain responses to acoustic tones and self-initiated finger movements. The frequency dependence of the amplitudes of these component responses may shed new light onto why spontaneous timing transitions occur in the first place. © 2000 Academic Press

1. INTRODUCTION

This paper follows previous work (Fuchs *et al.*, 1992; Kelso *et al.*, 1991, 1992), in which recordings of human magnetoencephalographic (MEG) activity were related to coordinated sensorimotor behavior. Subjects can syncopate a simple motor response (finger flexion) to a periodic auditory stimulus when the repetition frequency is low (<2 Hz) but fall into a synchronized response pattern at higher repetition rates. This well-known spontaneous switch in behavior from syncopation (anti-phase timing relation) to synchronization (in-phase) with an external metronome of increasing frequency has been used to probe for evidence of changes in neural activity patterns accompanying coordinative instability (Kelso *et al.*, 1990; Wimmers *et al.*, 1992). In previous studies, MEG signals were obtained with a 37-channel magnetometer located over the centrolateral area of the left hemisphere (contralateral to the response) and revealed three major findings:

1. The topography of the dominant spatial pattern of brain activity (obtained from a principal component analysis) changed at the transition frequency;
2. The dominant frequency of the corresponding time-dependent amplitude switched from the coordination frequency (prior to the transition) to twice the coordination frequency (after the transition);
3. The time-dependent amplitude also showed a shift of π that occurred contemporaneously with the behavioral phase transition in sensorimotor coordination.

Here we explore transitions in auditory–motor coordination using a 143-channel magnetometer that allowed for full-head coverage, thus providing access to cortical activity in both hemispheres at an enhanced spatial resolution. Additionally, the area covered by contralateral sensors was substantially larger than in the earlier experiment (outlined with white circles in Fig. 1). Our goals here are twofold: first, to replicate and extend the set of phenomena described above using more extensive sensor coverage and second, to explore, using additional techniques, the neurobiological origins of instability in this type of sensorimotor task by linking patterns observed during different coordinative timing relations (and transitions between them) to the more elementary events that constitute them, i.e., auditory and movement evoked fields and their interaction. We apply two procedures to decompose the spatiotemporal signals associated with performance of the coordination task into spatial patterns and corresponding time-dependent amplitudes. We then show how the primary activation patterns relate to the component sensory and motor events: we found that the activity prior to the transition is dominated by an auditory event-related field, whereas after the switch to synchronization, the pattern of largest amplitude corresponds to motor events. Around the behavioral transition the contributions of the two patterns assume similar values.

1053-8119/00 $35.00

2. METHODS

2.1. Experimental Procedure

Subjects were instructed to coordinate right finger flexion with a periodic series of auditory tones (1 kHz, 60-ms duration) in a syncopated fashion. Specifically, subjects ($N = 4$; 3 male, 1 female) were instructed to time the peak point of flexion in the middle of consecutive tones. A trial consisted of 80 tones (cycles) presented at eight different rates (plateaus), beginning at 1.0 Hz and increasing to 2.75 Hz in 0.25-Hz increments after every 10 cycles. This range of frequencies was chosen because it is known to induce spontaneous transitions to synchronization. The beginning of each trial was cued with three quick tones and a long tone (1-s duration) signaled the trial's end. Sixteen trials were collected for each subject.

Two control conditions were also included. In the auditory-only control, subjects listened to tones delivered with an interstimulus interval randomized between 2 and 4 s—a typical set-up for evoked responses. In the motor-only control, the subjects were instructed to perform self-initiated movements with the same movement profile used in the coordination experiment. They were further asked to pace the movements with interresponse intervals of approximately 3 s.

Subjects performed all conditions while seated inside a magnetically shielded room (Vacuum Schmelze, Hanau) with their heads held firm within a helmet containing the superconducting quantum interference devices (SQuIDs). The metronome was binaurally delivered through headphones at a volume that the subject reported to be comfortable. Responses were measured as pressure changes in a sensitive air pillow located just beneath the subject's right index finger and connected via 10 m of plastic tubing to a pressure-voltage transducer located outside of the shielded room. Subjects were asked to fixate at a point located approximately 2 m in front of them and to confine all eye movement to breaks between trials.

2.2. Data Acquisition

MEG activity was recorded at the General Hospital in Vienna, Austria using a multichannel full-head magnetometer (CTF Inc., Port Coquitlam). The magnetometer had 143 SQuID first-order gradiometers arranged in such a way that the scalp surface was uniformly covered. Conversion to third-order gradiometers was performed in firmware using a set of reference coils.

All signals (MEG, metronome, response) were bandpass filtered between 0.3 and 80 Hz and notch filters were set at the European line frequency and its harmonic, 50 and 100 Hz, respectively. They were then sampled at a rate of 312.5 Hz and digitally stored for further analysis. Due to the length of plastic tubing used to measure the response, the movement signal was subsequently corrected for a delay of 33 ms, the time to arrive at the transducer (given by the length of the tube divided by the speed of sound in air).

Prior to each trial the locations of three well-defined anatomical landmarks (fiduciary points), the nasion and the left and right preauricular points, were digitized. These three points were used to define the 3D coordinate system for sensor locations with respect to the subject's head.

2.3. Data Inspection and Segregation

Off-line all MEG and EEG signals were manually inspected for eye blinks and other artifacts. Contaminated data segments were marked and discarded from further analysis. Data from one of the male subjects were found to be extremely noisy due to dental fillings and were excluded from discussion in this paper.

Single cycles were classified as "syncopate" if the associated response fell within a range of $\pm 60°$ from the point midway between two tone onsets (i.e., 180°) and as "synchronized" if they were inside the same range relative to tone onset (i.e., 0° phase). All other cycles were omitted from further analysis. After this behavioral editing procedure, approximately 100–150 cycles per sensor, frequency, and subject remained and were averaged with respect to tone onset, yielding one time series per SQuID sensor, frequency plateau, and subject.

2.4. Single-Channel Analysis

Simple frequency decomposition of averaged waveforms was done with a discrete Fourier transform (DFT) to obtain power and phase spectra. The fundamental frequency always corresponded to the rate of coordination (i.e., plateau frequency) since averaging was done on a cycle basis. The relative phase of the brain signal in a single sensor was calculated from the Fourier transform as

$$\varphi = \arctan \frac{\Im(c_1)}{\Re(c_1)}, \tag{1}$$

where c_1 is the (complex) Fourier coefficient for the fundamental frequency, and $\Re(c_1)$ and $\Im(c_1)$ are its real and imaginary parts, respectively.

2.5. Spatiotemporal Analysis

To extract relevant information present in the time series from 143 sensors we apply two linear projection techniques, namely the Karhunen–Loève (KL) decomposition (also known as principal component analysis or PCA) and dual-basis projection. Both procedures separate the spatiotemporal dynamics into a spatial

part represented by (usually a few) spatial patterns and a temporal part, i.e., the amplitude of each of these pattern's evolution in time. In the case of the KL expansion both the spatial patterns and their amplitudes are calculated from the same data set and represent the dominant modes in the signal. However, the spatial patterns are restricted by orthogonality constraints and thus may not necessarily correspond to patterns that comprise the original signal set. On the other hand, the top spatial mode, i.e., the pattern accounting for the largest part of the signal variance, is not restricted to these orthogonality constraints and therefore may have a physiological interpretation (see e.g. Kelso *et al.*, 1998).

In contrast to the KL expansion the dual-basis projection uses a fixed set of basis vectors defined *a priori;* i.e., they are not calculated from the data set under consideration. For instance, here we decompose our data from the syncopate condition into patterns calculated from the auditory and motor-alone control conditions. These patterns, in general, are not orthogonal and they do not cover as much variance as the patterns from a KL expansion. However, they may be more physiologically relevant because they represent the brain response to the elementary events in our experiment, i.e., acoustic tones and finger movements. Again, the goal is to separate a spatiotemporal pattern $\mathbf{H}(t)$ into a spatial part and a temporal part but now the basis patterns are not necessarily orthogonal. Therefore, their time-dependent amplitudes cannot be calculated as a projection of the original signal onto these vectors but onto the corresponding adjoint vectors in dual space. Given a set of vectors $\phi^{(k)}$, the set of adjoint vectors is $\phi^{(k)+}$ with the property

$$\phi^{(k)} \cdot \phi^{(k')+} = \sum_{i=1}^{N} \phi_i^{(k)} \phi_i^{(k')+} = \delta_{kk'}. \tag{2}$$

In general, the number of basis vectors, M, will be much smaller than the number of components, N, for each vector (in our case we have $M = 2$ vectors with $N = 143$ components each) and (2) does not define the adjoint vectors uniquely. Therefore, we restrict the space for the adjoint vectors $\phi^{(k)+}$ to the subspace defined by the patterns $\phi^{(k)}$; i.e., we express the adjoint vectors as a linear combination of the vectors $\phi^{(k)}$, which reads in components

$$\phi_i^{(k)+} = \sum_{l=1}^{M} a_l^k \phi_i^{(l)}. \tag{3}$$

Inserting (3) into (2) we obtain

$$\sum_{i=1}^{N} \{\phi_i^{(k)} \sum_{l=1}^{M} a_l^{k'} \phi_i^{(l)}\} = \delta_{kk'}, \tag{4}$$

which represents a linear system of equations for the coefficients $a_l^{k'}$. By rearranging the sums, (4) can be written in the form

$$\sum_{l=1}^{M} a_l^{k'} \sum_{i=1}^{N} \phi_i^{(k)} \phi_i^{(l)} = \delta_{kk'}, \tag{5}$$

from which the coefficients $a_l^{k'}$ can be readily calculated. The time-dependent amplitudes $\xi_k(t)$ corresponding to the patterns $\phi^{(k)}$ are now given by

$$\xi_k(t) = \mathbf{H}(t) \cdot \phi^{(k)+} = \sum_{i=1}^{N} H_i(t) \phi_i^{(k)+}. \tag{6}$$

The system (5) has unique solutions only if the patterns $\phi^{(k)}$ are linearly independent. For practical applications it is estimated (Uusitalo and Ilmoniemi, 1997) that the angles α_{kl} between the patterns should not be smaller than 30° to produce meaningful results. If the patterns are normalized, these angles are given by

$$\alpha_{kl} = \arccos\{\sum_{i=1}^{N} \phi_i^{(k)} \phi_i^{(l)}\} \quad \text{with} \sum_{i=1}^{N} (\phi_i^{(j)})^2 = 1 \quad j = k, l. \tag{7}$$

The contribution of the pattern $\phi^{(k)}$ in the dual-basis projection can be defined as residuals of the mean square error

$$E^{(k)} = \frac{1}{\tau} \sum_{i=1}^{N} \int_0^T \{H_i(t) - \xi_k(t) \phi_i^{(k)}\}^2 dt \quad \text{with } \tau = \sum_{i=1}^{N} \int_0^T H_i^2(t) dt. \tag{8}$$

This error is a number between 0 and 1 and the corresponding contribution of pattern k is given as $k = 1 - E^{(k)}$. In order to obtain the total contribution to the variance in the original signal from M patterns we must calculate the quantity

$$\begin{aligned} \text{tot} &= 1 - E^{\text{tot}} \\ &= 1 - \frac{1}{\tau} \sum_{i=1}^{N} \int_0^T \{H_i(t) - \sum_{k=1}^{M} \xi_k(t) \phi_i^{(k)}\}^2 dt. \end{aligned} \tag{9}$$

For the case of an orthogonal set of basis vectors the quantities k and tot are identical to the eigenvalue λ_k and the sum of eigenvalues in the KL expansion, re-

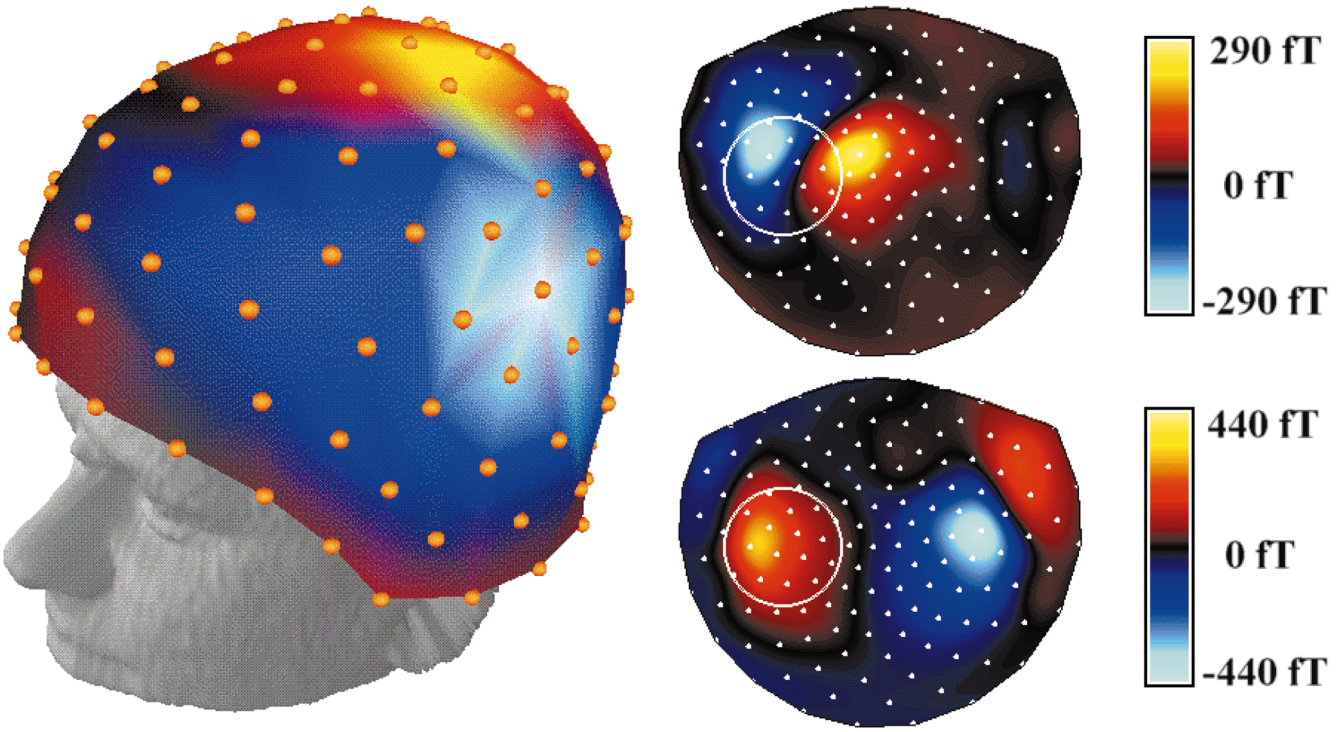

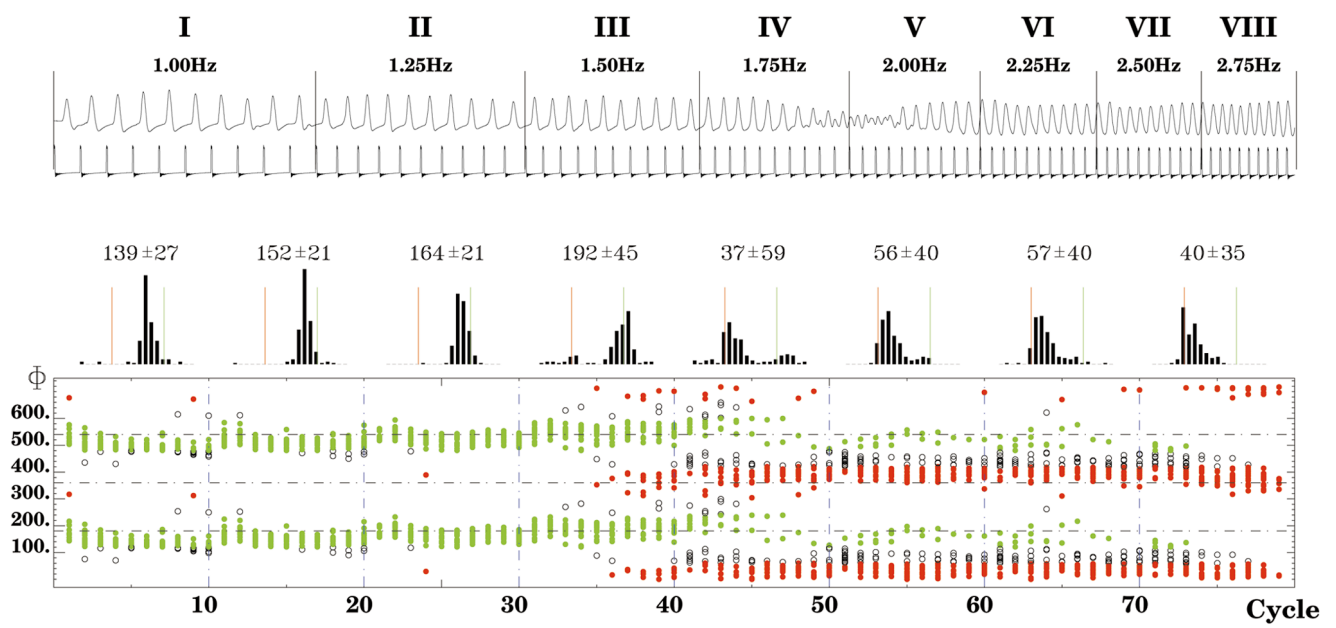

FIG. 1. Magnetic activity on a subject's head (left) and in polar projection (right). Red and yellow areas indicate where the magnetic field lines exit the head; in the blue regions the field lines enter. (Left) Subject's head reconstructed from an MRI scan with magnetic brain activity associated with a right finger movement superimposed. Maximum amplitude is located over the centrolateral area of the left hemisphere as expected. (Right top) The same activity pattern (motor-evoked field) projected into polar coordinates (the nose points up). The scale to the right shows the field amplitudes. Sensor locations used in the present experiment are indicated by dots; the circle shows the approximate area that was covered by the 37-channel device used in the earlier research (see Introduction). (Right bottom) Polar projection for an auditory evoked field.

FIG. 2. Relation between metronome and coordination behavior. (Top) Time series of metronome and response for an entire trial (averaged across trials from one subject). The switch in behavior can be seen around the border between plateaus IV and V. (Bottom) Corresponding relative phase (between response peak and tone onset) values plotted by cycle in a 4π diagram (all trials included). Cycles classified as syncopation are plotted in green, red indicates synchronization cycles, and all ommited cycles are open black. Histograms of relative phase values are plotted above together with the mean phase and standard deviation.

spectively. If the set is nonorthogonal, the value of tot may differ from the sum of the single contributions.

2.6. Topographic Displays

Throughout this article we will display magnetic brain activity as two-dimensional topographic plots (e.g., Fig. 1 (right)) in order to visualize the activity over the whole head as a single planar pattern. This 2D representation is obtained by projecting the 3D location of sensor i in spherical coordinates (r_i, θ_i, ϕ_i) into polar coordinates that define a location on a plane according to

$$X_i = s\theta_i \cos \phi_i \text{ and } Y_i = s\theta_i \sin \phi_i, \qquad (10)$$

where s is a scaling factor that determines the size of the topographic map. Figure 1 (right) shows two such representations for a sensorimotor (top) and an auditory-evoked field (bottom). White dots indicate the locations of the sensors. Data values between sensor locations were interpolated for topographic mapping with a 2D spline of third order.

3. RESULTS: COORDINATION BEHAVIOR

Figure 2 (top) shows the averaged time series for the metronome and finger movement on plateaus I–VIII for a representative subject. A transition from syncopated to synchronized coordination can be seen on plateaus IV and V. The presence of more than one response during the transition period is a result of averaging across trials and reflects the fact that subjects switched at different cycles in different trials. The bottom half of Fig. 2 shows the transition in terms of relative phase calculated between response peak and tone onset. Cycles classified as syncopation are plotted in green, synchronization cycles are in red, and those that did not fall into either category are indicated by black open circles. The distributions of relative phase values for each plateau are shown in the histograms with the mean $\pm$ standard deviation indicated for each distribution. The red and green lines in the histograms denote 0° (perfect synchronization) and 180° (perfect syncopation), respectively. It can be seen that, on average, when asked to syncopate the peak of the response was a bit early, whereas after the transition on plateau IV, response peaks are delayed with respect to tone onset rather than perfectly in-phase or synchronized. Nevertheless, there is a clear switch in coordination around the fifth plateau.

4. RESULTS: SPATIOTEMPORAL DYNAMICS OF MEG ACTIVITY

4.1. Control Conditions: Auditory and Motor Evoked Fields

Shown in Fig. 3 are time series of averaged MEG activity from the two control conditions. The top half shows the response evoked by an auditory tone and on the bottom, that for a voluntary finger flexion. The number of events in these averages is approximately 80. Overlaid is the topographic pattern at maximum amplitude that occurs at 92 ms after stimulus onset for the auditory event and at 20 ms prior to peak movement amplitude for the sensorimotor case. Regions of strong activity are overlaid in orange–yellow denoting magnetic field lines exiting the head (at the time of maximum brain activity) and in light blue where the field lines enter. The auditory event elicits two dipolar patterns, one over each hemisphere with the one over the right side more pronounced. The motor field is a single dipole over the left hemisphere contralateral to the right-handed finger movement. The maximum amplitudes are 440 and 290 fT for the auditory and movement evoked fields, respectively.

4.2. The Syncopate Condition

Figure 4 shows the time series of magnetic activity averaged over trials and cycles for the syncopate condition at coordination frequencies of 1.25 Hz (plateau II) before the transition and 2.5 Hz (plateau VII) after the transition. Overlaid are the patterns that correspond to maximum field amplitude that occurred at 90 and 45 ms after stimulus onset for plateaus II and VII, respectively.

On plateau II two dipolar fields exist, one in each hemisphere. This pattern reflects the brain's auditory response, as is evident from a comparison with the auditory control (Fig. 3). Later in the cycle there is a second peak that reflects movement (see also Fig. 5). On plateau VII the activity over the right hemisphere seen on plateau II has disappeared almost completely. The remaining field over the left hemisphere is dipolar and the pattern and the time series are very similar to the motor-only control in Fig. 3. Note that the time series are shifted compared to the motor-only control condition because in Fig. 3 signals are averaged with respect to peak amplitude (as there is no stimulus), whereas the data on plateau VII are averaged with respect to stimulus onset. The relation between stimulus and movement is plotted on the lower right corner of Fig. 4, showing that the peak movement occurs after stimulus onset (about 70 ms), which accounts for this shift in time.

Topographic sequences (sampled every 64 ms) are shown in Fig. 5. Plotted below each topo are the time series of the stimulus (green) and movement response (blue). The red vertical line indicates the location of the topo within the cycle. On plateau II an auditory pattern appears shortly after the stimulus (visible at the end of first and start of the second row). The polarity of this pattern reverses at the start of the third row and at the end of this row a movement-related dipolar pattern over the left hemisphere becomes visible. Com-

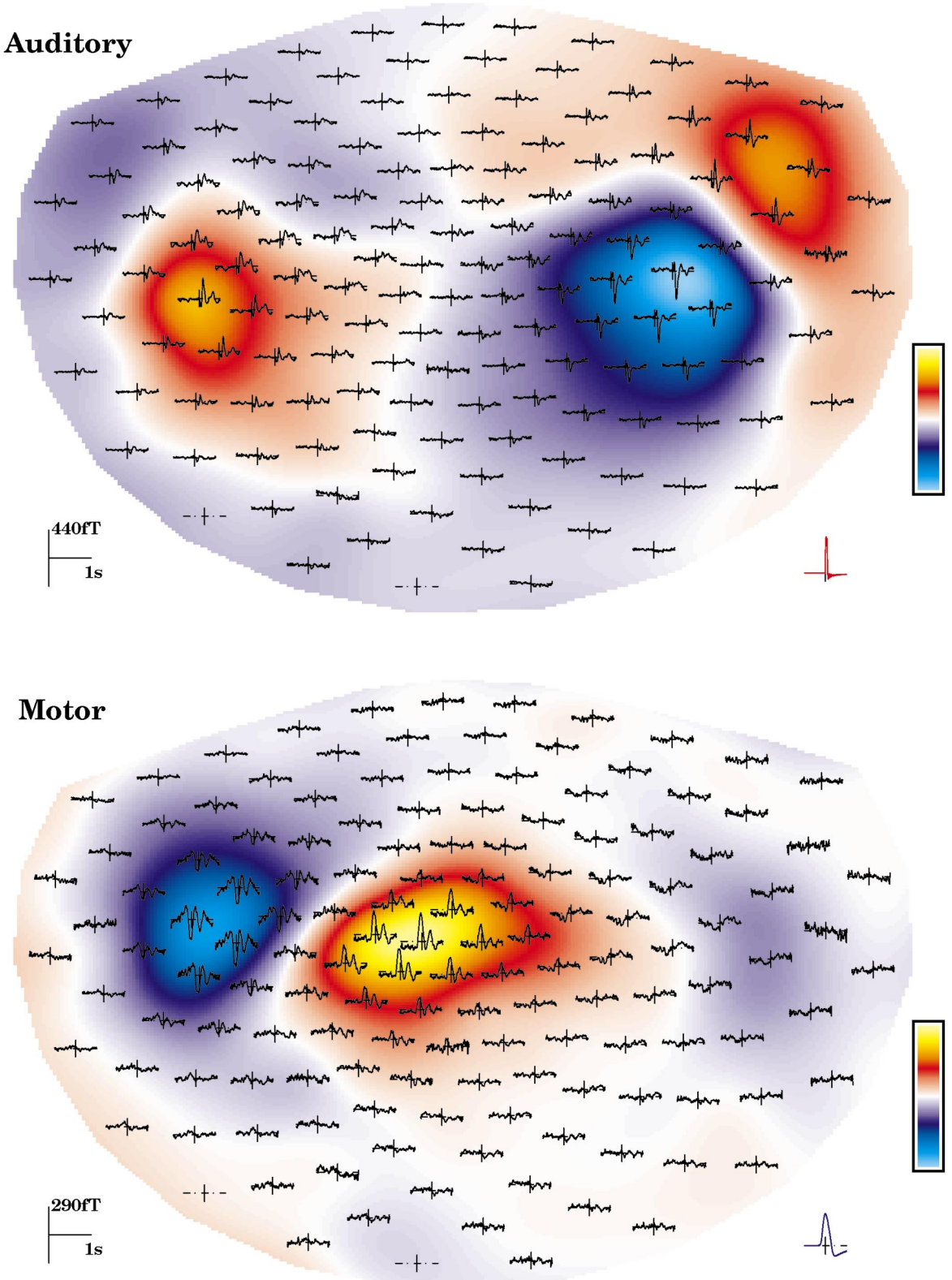

FIG. 3. Control conditions: Time series of magnetic brain evoked activity by an auditory tone (top) and flexion of the right index finger (bottom) overlaid with topographic patterns corresponding to the maximum field amplitude (93 ms after tone onset for the auditory control and 22 ms prior to peak flexion for the motor control). In the lower right of each subplot the time series for the stimulus (top) and the movement profile (bottom) are shown.

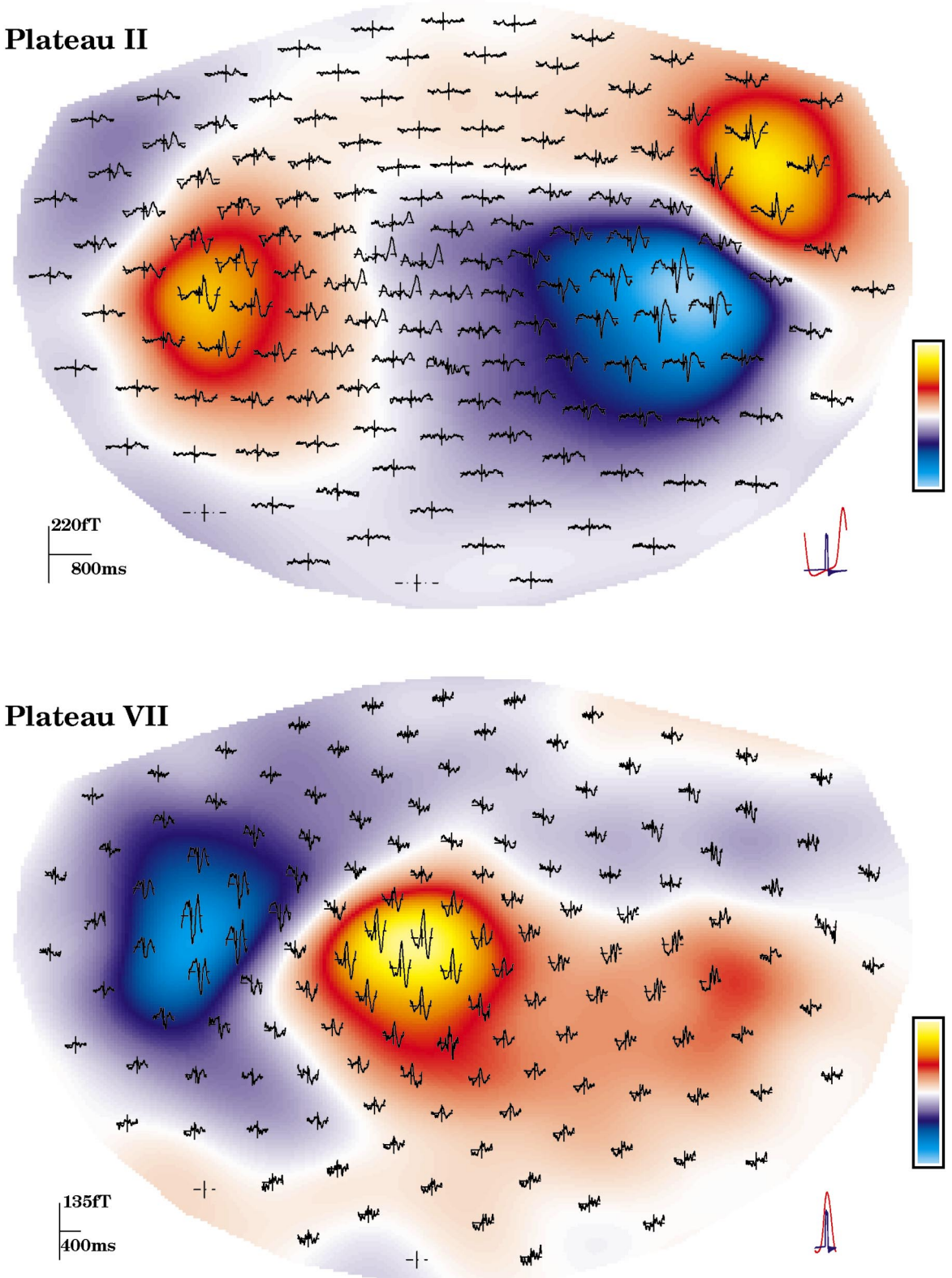

FIG. 4. Time series of magnetic brain activity in single channels in topographic sensor layout for the syncopate condition on plateau II (top) before the transition and plateau VII (bottom) posttransition overlaid with the spatial patterns at the time of maximum activity (90 and 45 ms after stimulus onset for plateaus II and VII, respectively). In the lower right of each subplot time series for the metronome and the movement are shown for a syncopate (top) and a synchronized cycle (bottom).

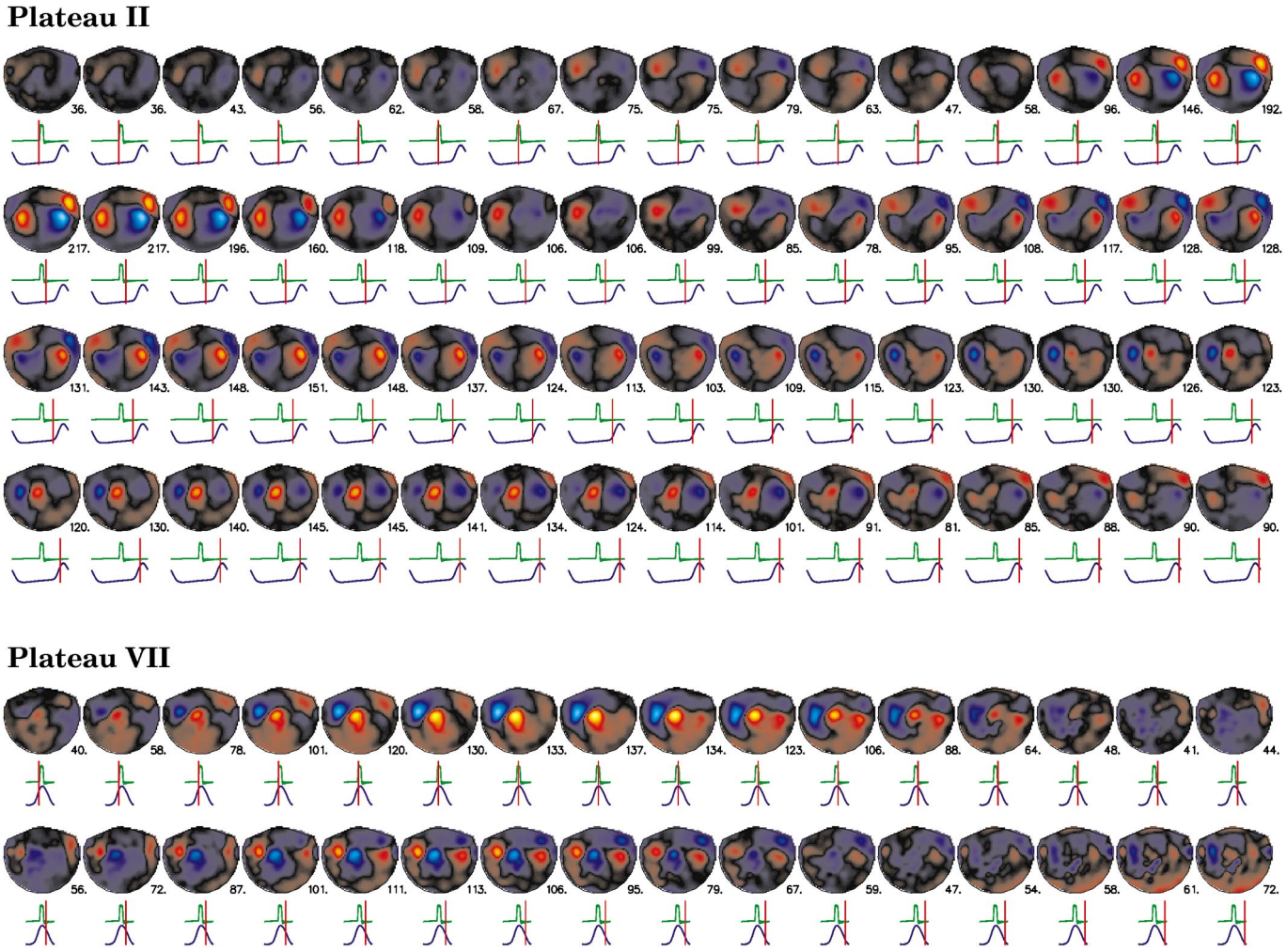

FIG. 5. Sequences of topographic plots of magnetic brain activity on plateaus II and VII sampled every 64 ms. Plotted below each topo are the time series of the stimulus (green) and response (blue). The red vertical line indicates the location of the topo within the cycle. The number next to the topo is the maximum activity at this time point in fT.

pared to the auditory pattern the amplitude of the pattern over sensorimotor cortex is small as is to be expected from inspection of the control conditions (cf. Fig. 3).

On plateau VII the dominant pattern is the movement dipole that appears shortly before peak amplitude reaches a maximum and then reverses in polarity in the second row for this plateau. Activity over the right hemisphere is hardly visible at the beginning of the second row. Notice that the overall amplitude on plateau VII is smaller than on plateau II and that the motor dipole oscillates at twice the stimulus frequency; i.e., it performs a complete oscillation for the half cycle that is shown.

The frequency components for these time series are shown in the power spectra depicted in Fig. 6 for the same pre- and posttransition plateaus overlaid with the spatial pattern of total power. On plateau II power is distributed over both hemispheres and most of the spectra are broad, i.e., do not show a dominant frequency. On plateau VII activity over auditory areas has virtually disappeared and the motor dipole oscillates at twice the coordination rate as indicated by the dominant spectral component at this frequency.

Plots of the relative phase between the stimulus and the time series of the brain signal calculated from the Fourier component at the coordination frequency on all eight plateaus (Fig. 7) show a jump by a value of π mainly over the left hemisphere in areas where the motor field is strong. In Fig. 7 larger solid circles indicate that the power at the coordination frequency in a given channel was larger than 5% of the maximum power on at least one plateau. Smaller open circles were used when the largest power was smaller than this value. In the left half of the motor dipole the phase switches from $-\pi$ to 0, whereas in the right half the switch is from 0 to π. This difference is due to fact that the time series in both halves of the left dipole have

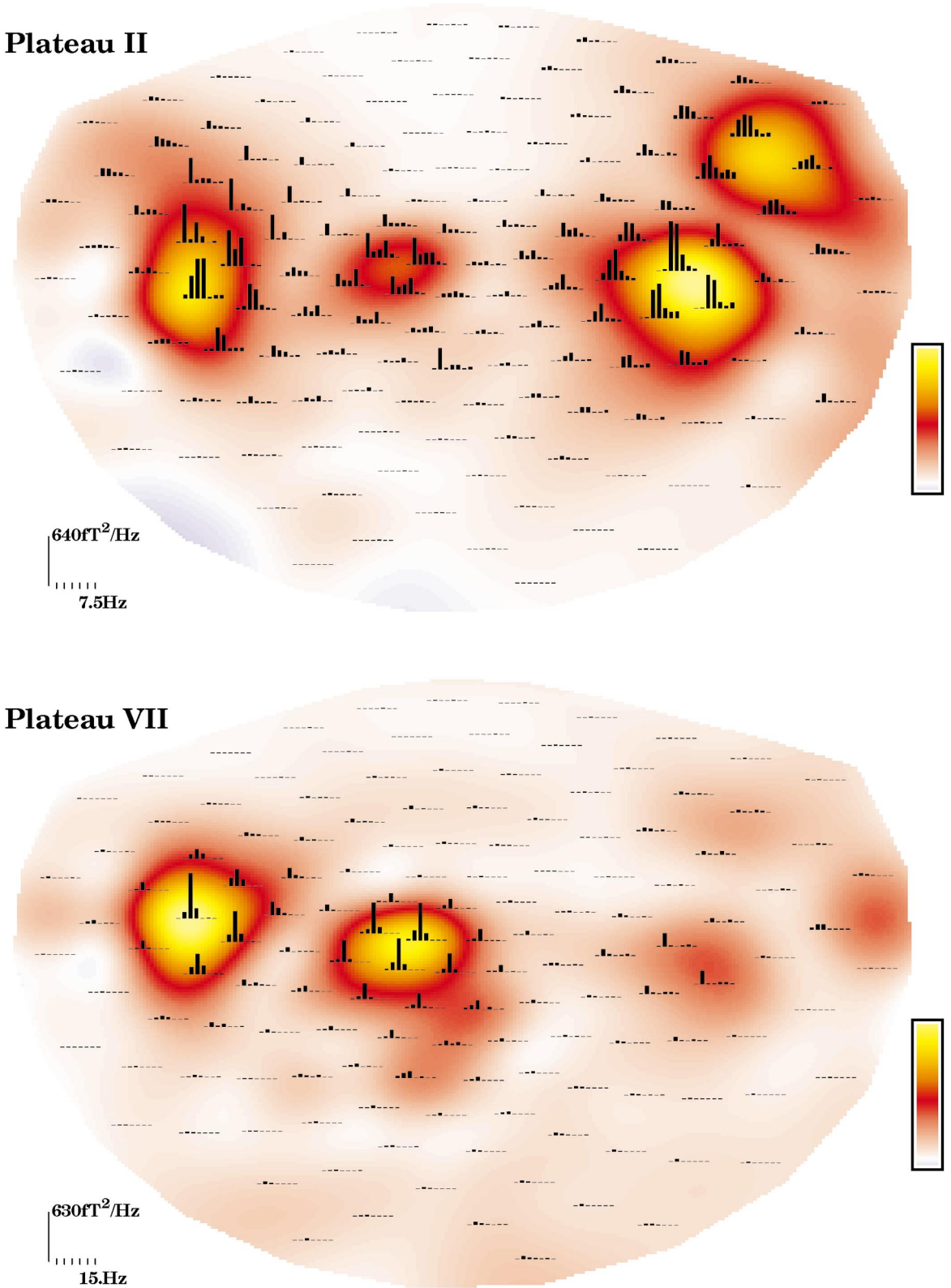

FIG. 6. Power spectra obtained from the time series for the syncopate condition on plateau II (top) and plateau VII (bottom) overlaid with the spatial patterns representing the total power.

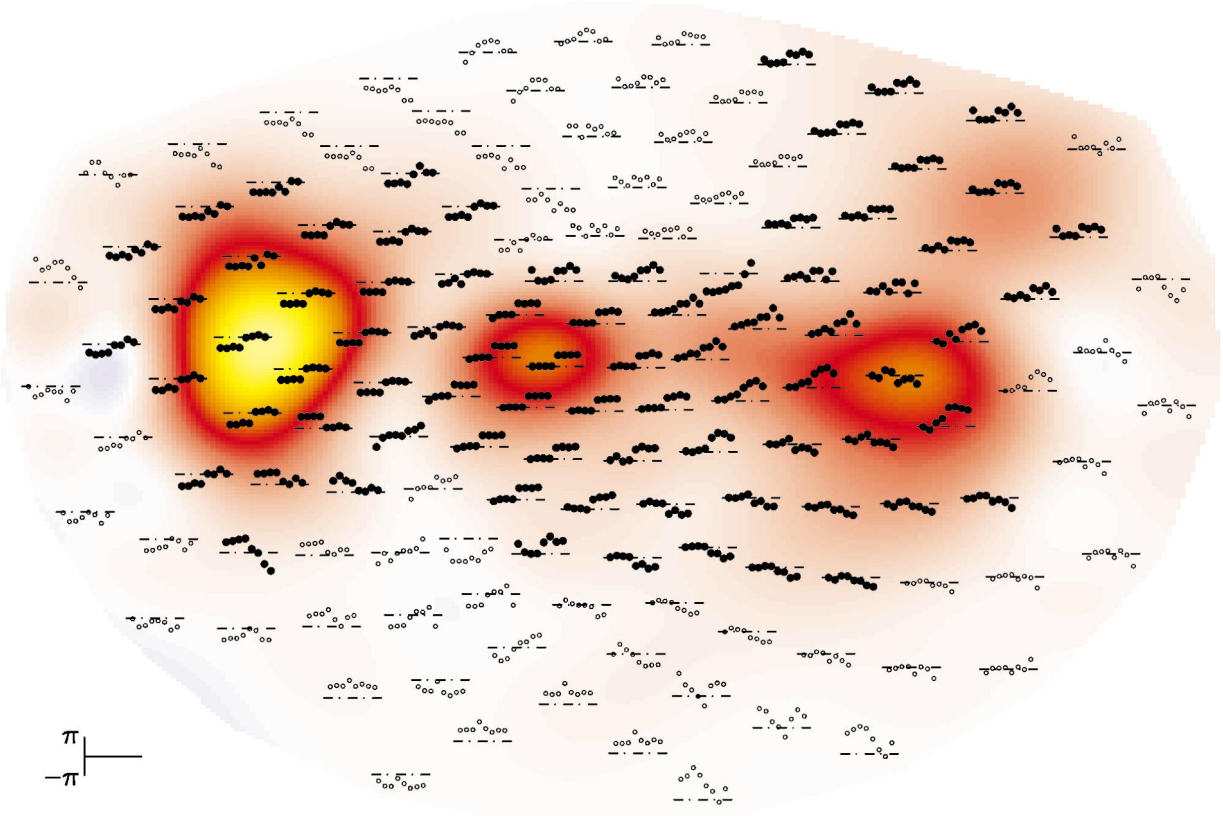

FIG. 7. Relative phase between the stimulus and the brain signal for the syncopate condition on all eight plateaus overlaid with the spatial patterns representing the power of the largest Fourier component at the coordination frequency. Larger solid circles indicate that the power at the coordination frequency in this channel was larger than 5% of the largest power on at least one plateau. Smaller open circles were used when the largest power did not exceed this value.

essentially the same shape but are reversed in polarity. Other cortical areas are characterized by little or no signal (e.g., sensors over frontal and occipital regions) or high amplitude, but little or no relation to the task (e.g., ipsilateral motor and temporal regions).

5. DECOMPOSITION OF SPATIOTEMPORAL DYNAMICS OF THE BRAIN

KL expansions for the auditory and motor-only control conditions are shown in Fig. 8. Like the pattern at maximum amplitude (Fig. 3) the dominant mode in the auditory control shows dipoles over the right and (less pronounced) left hemispheres. The corresponding amplitude has its main peak about 100 ms after stimulus onset. The dominant pattern from the motor alone condition is a single dipole over the contralateral hemisphere. Notice that the polarity is reversed compared to Fig. 3. We chose this representation because it simplifies the comparison with the patterns obtained from the syncopate condition (see below). The time course of the amplitude has the typical shape for a voluntary movement (e.g., Cheyne and Weinberg, 1989; Kristeva *et al.*, 1991) with a slow build-up of the readiness field prior to movement onset, the peak of the premotor field, the three motor-evoked fields with reversed polarity, and the postmotor field after the movement.

Figure 9 shows the first two spatial patterns, their corresponding amplitudes, and spectra of the time series for all eight plateaus of the syncopate condition. The dominant mode on the first three plateaus is very similar to the auditory control with dipolar activity over both hemispheres. The time series is also similar to the auditory control with a peak approximately 100 ms after stimulus onset followed by a smaller amplitude second peak with reversed polarity after about 200 ms. As the coordination frequency increases this reversed peak becomes almost the same size as the first peak, beginning on plateau III. On plateau IV the pattern becomes more movement-like and the time series no longer exhibits a sharp peak after the stimulus. On plateaus V–VIII, i.e., after the transition to synchronization is complete, the motor pattern dominates and the time series shows the pronounced minimum around the middle of the cycle where stimulus and peak movement coincide. On posttransition pla-

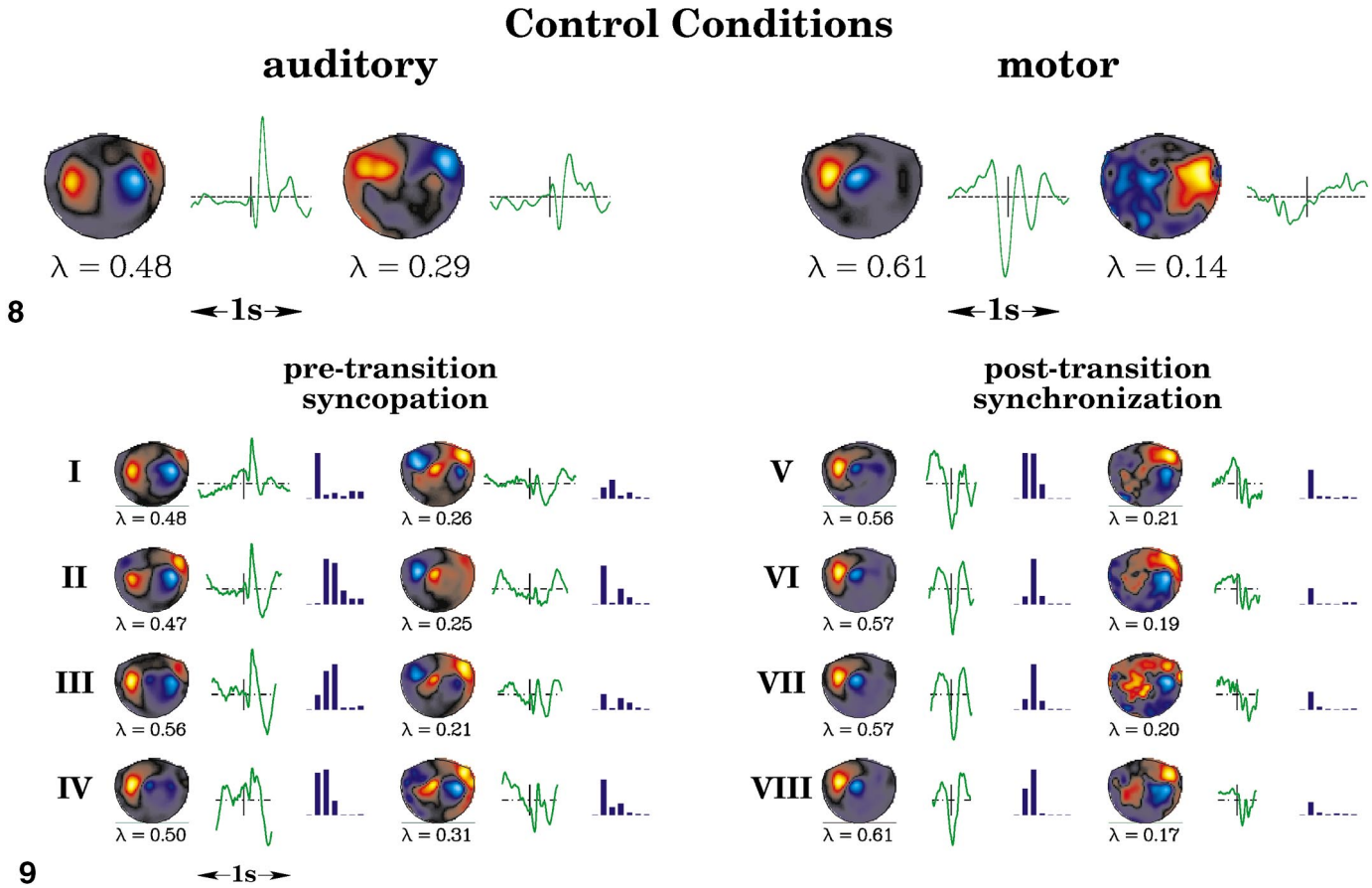

FIG. 8. The first two modes and their amplitudes from KL decompositions for the auditory and motor alone control conditions.
FIG. 9. The first two modes and their amplitudes from KL decompositions for the syncopate condition on all plateaus.

teaus the contribution of the second modes is smaller compared to pretransition values, whereas the eigenvalue for the first mode increases slightly. This indicates a spatiotemporal signal that is more dominated by a single spatial distribution of brain activity.

A dual-basis projection from the syncopate condition into the patterns from the auditory (top) and movement (bottom) control conditions is shown in Fig. 10. On the left, the spatial patterns (left column) and their adjoints (right column) are plotted. The strong similarity between the patterns and their adjoints indicates that the auditory- and movement-related patterns are almost orthogonal. The angle calculated from (7) for these two patterns turns out to be 71°. The time series corresponding to the auditory pattern (top row) exhibits the typical shape for an evoked event on the pretransition plateaus (I–IV). The relative amplitude indicated as a number next to the time series decreases on these plateaus as the coordination frequency increases. Posttransition (plateaus V–VIII) activity with an auditory spatial distribution is virtually absent and the time series are quite noisy. Power spectra plotted below the time series do not show an especially consistent behavior across frequency plateaus.

The time series corresponding to the motor pattern display a qualitative change at the transition point. Pretransition, the largest (negative) amplitude is located around the beginning and the end of the cycle and switches to the center position on posttransition plateaus (the locations where the movement actually occurs). The relative amplitude shows no significant dependence on the coordination frequency. The contribution of both patterns to the total variance of the magnetic brain activity (given by the value of tot) stays almost constant around 65% on all plateaus, whereas the relative contributions from auditory- and motor-related activity (denoted by the values of k for the two patterns) change significantly across frequency. That is, the amplitude of the auditory component normalized to a maximum of 1 (shown next to the time series) decreases systematically across plateaus, whereas the amplitude for the movement component is about constant. The power spectra below the time series exhibit a strong to dominant component at the coordination frequency on pretransition plateaus, whereas post-

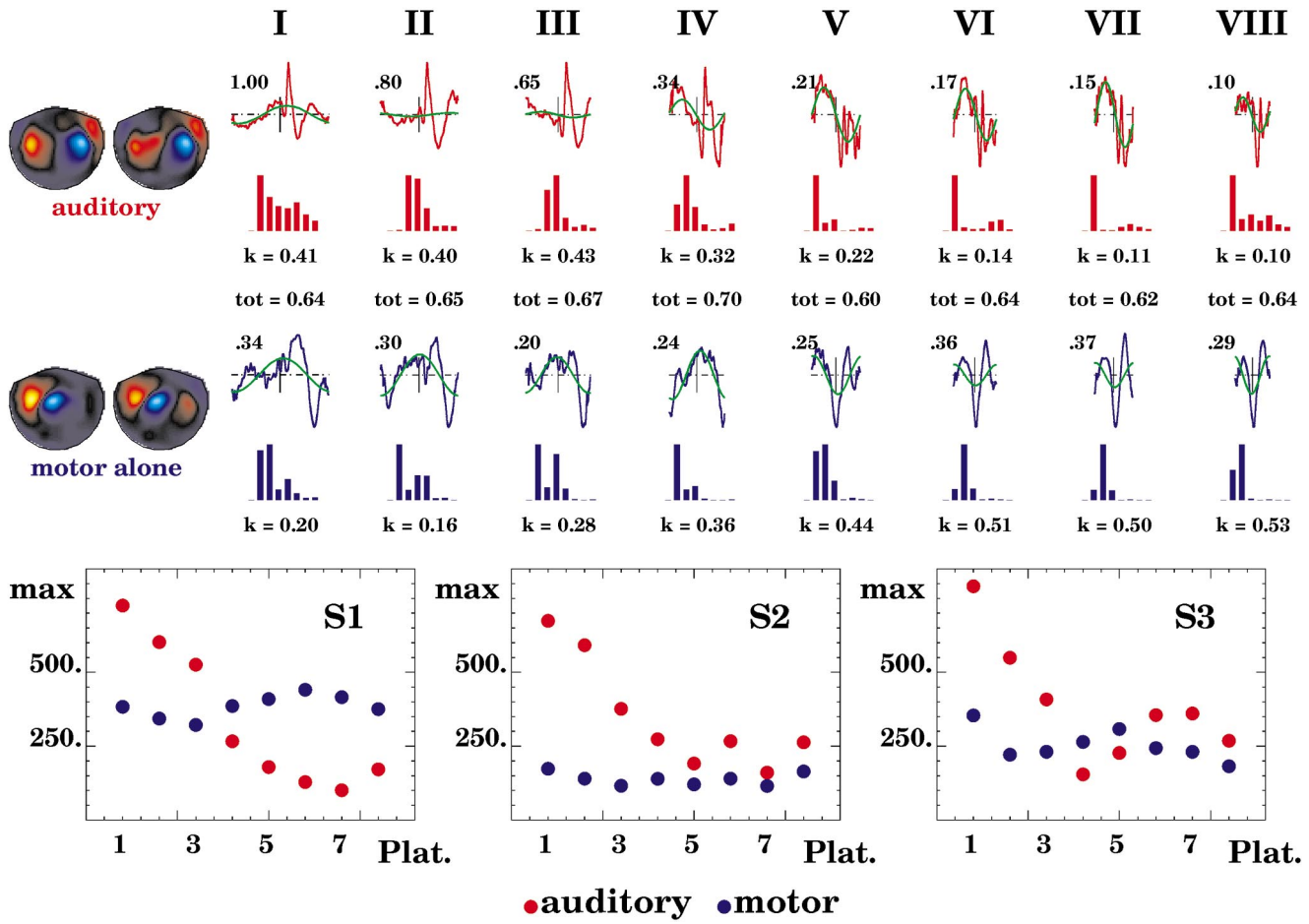

FIG. 10. Dual-basis projection of the syncopate condition into a basis composed of the auditory and motor-only control conditions (see text).

FIG. 11. Peak amplitudes of the decomposition for the syncopate condition into the auditory (red) and motor (blue) basis pattern for all subjects. As coordination frequency increases the auditory pattern drops out, whereas the motor related amplitude remains approximately constant.

transition the first harmonic at twice this rate dominates. Overlaid on the time series (in green) is the function that corresponds to the Fourier component at the coordination frequency that shows the phase shift of π at the transition point between plateaus IV and V. The same (green) time series for the auditory pattern shows no well-defined phase in the pretransition region. Posttransition, the phase is consistently around $\pi/2$ even though the overall amplitude is small.

This amplitude dependence for the auditory and movement components as a function of coordination frequency is shown for all three subjects in Fig. 11. Plotted is the peak (normalized) amplitude for the auditory (red) and movement (blue) patterns across plateaus. The movement-related amplitude stays approximately constant, whereas the amplitude of the auditory pattern decreases almost linearly with frequency on pretransition plateaus converging to a small constant value posttransition.

6. DISCUSSION AND CONCLUSIONS

The present study used a full-head SQuID array to investigate the spatiotemporal dynamics of neuromagnetic activity and their relation to a well-defined behavioral transition from syncopated to synchronized auditory–motor coordination. Our results allow physiological interpretations of three phenomena that were not previously possible due to limited sensor coverage. We had previously reported (Fuchs *et al.*, 1992; Kelso *et al.*, 1992) that the dominant spatial pattern of brain activity changes at the transition point. Now we can interpret this change as a switch from a bilateral auditory field pattern to a contralateral motor field. This happens because auditory-related brain activity decreases in amplitude with increasing frequency, whereas the contribution from sensorimotor cortical sources stays roughly constant throughout. Although auditory event-related potentials and event-related

fields (Hari *et al.*, 1982; Näätänen and Picton, 1987) have been previously studied in the low-frequency range, i.e., with interstimulus intervals between 1 and 16 s, the frequency range in our experiment (interstimulus intervals between 1 s and 400 ms), to our knowledge, has not been investigated systematically. However, preliminary results show a similar drop in amplitude of the auditory-like pattern as stimulus frequency increases (Carver *et al.*, 1999). The virtual disappearance of auditory activity at higher frequencies also explains our previous result (Fuchs *et al.*, 1992) that pre- and posttransition activity cannot be obtained by superimposing auditory and motor-only fields from control conditions with different phase lags.

From the dual-base decomposition it is also clear now that the emergence of oscillations at twice the coordination frequency after the transition is due to the dominance of sensorimotor activity. Time-dependent amplitudes for the motor pattern at high plateaus are characterized by an almost sinusoidal waveshape with two peaks per cycle. In contrast, at low plateaus features of event-related fields associated with transient voluntary movement can be identified. These include a slow readiness field prior to movement (e.g., plateau 2, Fig. 10) followed by a series of evoked components. The lack of a readiness field posttransition is notable as it may reflect a change in motor planning mechanisms.

As far as the π shift in the phase of the brain signal is concerned, we conclude that it is solely related to the switch in timing of the motor response. We base this conclusion on two observations. First, the coordination frequency component of the time-dependent amplitudes of the motor dipole shift by π at the transition as can be seen in Fig. 10. Second, only sensors over the contralateral sensorimotor area show this shift in the event-related fields; it is not evident over other areas of the head.

Our results thus demonstrate that the reorganization of the coordinative pattern on the behavioral level is accompanied by changes in the spatiotemporal dynamics of auditory and motor cortical activity. Whereas the phase shift in the brain signal appears to reflect the fact that a behavioral transition has already occurred (i.e., the motor response and hence the motor dipole component of the event-related fields has shifted in time), it is not clear whether the changes in the auditory response and motor field waveshape are dependent on the occurrence of this transition. A more likely explanation is that they reflect changes in the neural response to auditory and motor events of increasing rate. These frequency-dependent changes may in fact contribute to the increasing instability of syncopation by leading to changes in sensorimotor integration processes that cause entrainment of the motor response to the metronome. For example, a readiness field is observed when humans perform intentional movements and may be necessary to separate finger flexion from each auditory tone. Synchronization, on the other hand, is more automatic and less intention or planning may be necessary to keep pace with the metronome.

In conclusion, a key idea in this experiment is that emergent macroscopic patterns of neural activity form and spontaneously reorganize under continuous changes in a system-sensitive parameter, here the coordination frequency (Fuchs *et al.*, 1992; Kelso *et al.*, 1992; Mayville *et al.*, 1999; Wallenstein *et al.*, 1995). Generally speaking, such functional reorganization and change are due to instability in the spatiotemporal dynamics: under parametric variation, a given pattern of coordination among individual components becomes unstable and switches to a new form of coordination. Instability is a sign of so-called self-organization in behavioral and neural systems. Whereas the generic features of instability in self-organized dynamical systems are now commonplace (e.g., enhanced fluctuations and critical slowing down prior to the transition; see Haken (1996); Kelso (1995); Schöner and Kelso (1988) for review), the specific physiological mechanisms underlying phase transitions in brain and behavior are still unclear. The results presented here may signify a central mechanism underlying transitions from syncopated to synchronized unimanual coordination with an external metronome that involves a dynamic reorganization of neural activity in auditory and motor-related cortical areas. This is in contrast to other work that suggests that the physiological mechanism through which instability arises in this type of coordination task is at the neuromuscular–skeletal level (Carson *et al.*, 1999; see also Kelso *et al.*, submitted for publication, for a reply).

Future work is needed to clarify the relation between auditory and motor neuromagnetic responses and the mode of coordination on the behavioral level by examining, for example, situations in which the frequency is increased but transitions in coordinative timing do not occur.

ACKNOWLEDGMENTS

Research supported by NIMH (Neurosciences Research Branch) Grant MH42900, KO5 MH01386 to JASK, and the Human Frontier Science Program. We thank the MEG group at the AKH in Vienna for their hospitality, and Gerald Lindinger and Dagmar Mayer for their help during the data collection.

REFERENCES

Carson, R. G., Byblow, W. D., Poon, P., and Smethurst, C. J. 1999. Changes in posture alter the attentional demands of voluntary movement. *Proc. R. Soc. London B* **266:**853–857.

Carver, F. W., Fuchs, A., Mayville, J. M., Davis, S. W., and Kelso, J. A. S. 1999. Systematic investigation of the human brain's response to rhythmic auditory stimulation. In *Dynamical Neuro-*

science VII, Satellite Symposium at the Annual Meeting of the Society for Neuroscience, Miami, October 1999.

Cheyne, D., and Weinberg, H. 1989. Neuromagnetic fields associated with unilateral finger flexions: Pre-movement and movement-evoked fields. *Exp. Brain Res.* **78:**604–612.

Fuchs, A., Kelso, J. A. S., and Haken, H. 1992. Phase transitions in the human brain: Spatial mode dynamics. *Int. J. Bifurc. Chaos* **2:**917–939.

Haken, H. 1996. *Principles of Brain Functioning: A Synergetic Approach to Brain Activity, Behavior and Cognition*. Springer Verlag, Berlin.

Hari, R., Katila, K., Tumiomisto, T., and Varpula, T. 1982. Interstimulus interval dependence of the auditory cortex response and its magnetic counterpart: Implications for their neural generation. *Elec. Clin. Neuro.* **54:**561–569.

Jirsa, V. K., Friedrich, R., Haken, H., and Kelso, J. A. S. 1994. A theoretical model of phase transitions in the human brain. *Biol. Cybern.* **71:**27–35.

Jirsa, V. K., and Haken, H. 1997. A derivation of a macroscopic field theory of the brain from the quasi-microscopic neural dynamics. *Physica D* **99:**503–526.

Jirsa, V. K., Fuchs, A., and Kelso, J. A. S. 1998. Connecting cortical and behavioral dynamics: Bimanual coordination. *Neural Comput.* **10:**2019–2045.

Kelso, J. A. S. 1995. *Dynamic Patterns: The Self-Organization of Brain and Behavior.* MIT Press, Cambridge, MA.

Kelso, J. A. S., DelColle, J. D., and Schöner, G. 1990. Action–perception as a pattern forming process. In *Attention and Performance XIII* (M. Jeannerod, Ed.), pp. 139–169. Erlbaum, Hillsdale, NJ.

Kelso, J. A. S., Bressler, S. L., Buchanan, S., DeGuzman, G. C., Ding, M., Fuchs, A., and Holroyd, T. 1991. Cooperative and critical phenomena in the human brain revealed by multiple SQUIDs. In *Measuring Chaos in the Human Brain* (D. Duke and W. Pritchard, Eds.), pp. 97–112. World Scientific, Singapore.

Kelso, J. A. S., Bressler, S. L., DeGuzman, G. C., Ding, M., Fuchs, A., and Holroyd, T. 1992. A phase transition in human brain and behavior. *Phys. Lett. A* **169:**134–144.

Kelso, J. A. S., Fuchs, A., Lancaster, R., Holroyd, T., Cheyne, D., and Weinberg, H. 1998. Dynamic cortical activity in the human brain reveals motor equivalence. *Nature* **392:**814–818.

Kelso, J. A. S., Fuchs, A., and Jirsa, V. K. 1999. Traversing scales of brain and behavioral organization I–III. In *Analysis of Neurophysiological Brain Functioning* (C. Uhl, Ed.), pp. 73–125. Springer Verlag, Berlin.

Kelso, J. A. S., Fink, P. W., and DeLaplain, C. R. Submitted for publication. Haptic information stabilizes and destabilizes coordinated movement: A reply to Carson *et al.* (1999).

Kristeva, R., Cheyne, D., and Deecke, L. 1991. Neuromagnetic fields accompanying unilateral and bilateral voluntary movements: Topography and analysis of cortical sources. *Elec. Clin. Neuro.* **81:** 284–298.

Mayville, J. M., Bressler, S. L., Fuchs, A., and Kelso, J. A. S. 1999. Spatiotemporal reorganization of electrical activity in the human brain associated with a timing transition in rhythmic auditory–motor coordination. *Exp. Brain Res.* **127:**371–381.

Näätänen, R., and Picton, T. 1987. The N1 wave of the human electric and magnetic response to sound: A review and analysis of the component structure. *Psychophysiology* **24**(4):375–425.

Schöner, G., and Kelso, J. A. S. 1988. Dynamic pattern generation in behavioral and neural systems. *Science* **239:**1513–1520.

Uusitalo, M. A., and Ilmoniemi, R. J. 1997. Space-signal projection method for separating MEG or EEG into components. *Med. Biol. Eng. Comput.* **35:**135–140.

Wallenstein, G. V., Kelso, J. A. S., and Bressler, S. L. 1995. Phase transitions in spatiotemporal patterns of brain activity and behavior. *Physica D* **84:**626–634.

Wimmers, R. H., Beek, P. J., and van Wieringen, P. C. W. 1992. Phase transitions in rhythmic tracking movement: A case of unilateral coupling. *Hum. Movement Sci.* **11:**217–226.